RSC Advances

This is an *Accepted Manuscript*, which has been through the Royal Society of Chemistry peer review process and has been accepted for publication.

Accepted Manuscripts are published online shortly after acceptance, before technical editing, formatting and proof reading. Using this free service, authors can make their results available to the community, in citable form, before we publish the edited article. This *Accepted Manuscript* will be replaced by the edited, formatted and paginated article as soon as this is available.

You can find more information about *Accepted Manuscripts* in the Information for Authors.

Please note that technical editing may introduce minor changes to the text and/or graphics, which may alter content. The journal's standard Terms & Conditions and the Ethical guidelines still apply. In no event shall the Royal Society of Chemistry be held responsible for any errors or omissions in this *Accepted Manuscript* or any consequences arising from the use of any information it contains.

ROYAL SOCIETY OF CHEMISTRY

www.rsc.org/advances

RSC Advances

ARTICLE

Fabrication of Transparent Conducting Ni-Nanomesh-Embedded Film Using Template-Assisted Ni Electrodeposition and Hot Transfer Process

Received 00th January 20xx,
Accepted 00th January 20xx

DOI: 10.1039/x0xx00000x

www.rsc.org/

Hak-Jong Choi, Sang-woo Ryu, Junho Jun, Sungjin Moon, Daihong Huh, Yang Doo Kim, Heon Lee*

In the present work, we developed a new method for fabricating Ni nanomeshes for transparent conducting electrodes using template-assisted Ni electrodeposition and a hot transfer process. By employing the direct printing of hydrogen silsesquioxane (HSQ), the microscale HSQ template was successfully transferred onto a stainless steel substrate. The Ni nanomesh was fabricated using selective Ni electrodeposition and a hot transfer process on a polycarbonate (PC) film. The Ni-nanomesh-embedded PC film exhibited approximately 77% of the transmittance compared to that of the PC film and a sheet resistance of 2–10 Ω/sq. In addition, the transmittance and sheet resistance of the Ni-nanomesh-embedded PC film was not significantly degraded after 20,000 cycles of bending tests.

Introduction

Transparent conducting electrodes (TCEs) have attracted much attention as an essential element of various optoelectronic devices such as photovoltaics (PVs),[1,2] organic light-emitting diodes (OLEDs),[3] touch-screen panels (TSPs),[4] radiofrequency identification (RFID),[5] and liquid crystal displays (LCDs).[6] At the commercial level, indium tin oxide (ITO) and fluorine-doped tin oxide (FTO) have been used as TCEs of optoelectronic devices because of their good optical and electrical properties such as high optical transmittance and low electrical resistance.[7–9] However, oxide-based TCEs exhibit the inherent drawbacks of brittleness, a high refractive index, a low optical transmittance for UV, and a high-temperature process limited to apply to various devices such as UV-operated devices or flexible and bendable devices.[10–12]

As a result, many researchers have investigated alternative TCEs such as graphene,[13,14] carbon nanotubes (CNTs),[15] metal (Ag, Cu) nanowires (NWs),[16–18] metal meshes,[19,20] and conducting polymers[21] for flexible TCEs. Compared with ITO, however, carbon-based TCEs such as graphene, CNTs, and conducting polymers exhibit relatively poor optical and electrical properties.[22] In case of metal NWs, Ag NWs with excellent electrical and optical properties have been recently developed; however, the mass production of Ag NWs is limited by their scarcity and price ($505 USD/kg).[23] Metal meshes have also attracted because of their superior optical and electrical properties similar to metal NWs. In addition, metal meshes also have the advantages of uniformity of electrical spreading compared with a metal NW network.[24] In addition, the transmittance and resistance can be easily controlled by tuning the parameters of the metal mesh such as the pitch and linewidth. For these reasons, many researchers have already developed methods for metal meshes such as lithography and evaporation,[25] nanotransfer printing,[26] anodic aluminum membrane[27] and direct patterning of Ag nanoparticles (NPs).[28] However, these methods have some limitations in the control of electrical properties, fabrication costs, and processes on flexible substrates.

In this study, we introduce a cost-effective and controllable method for fabricating Ni-nanomesh-based TCEs on flexible film using template-assisted Ni electrodeposition and a hot transfer process. The height of the Ni nanomesh was controlled by tuning the Ni deposition time. Three different heights of Ni nanomeshes were investigated in terms of the resulting optical and electrical properties. In addition, we confirmed the surface morphology and current flow of the Ni nanomesh. Finally, the bending resistance of Ni nanomesh was investigated by performing bending tests for 20,000 cycles.

Experimental

Fabrication of Ni-nanomesh-embedded film.

Fig. 1 presents a schematic illustration of the fabrication process of the Ni-nanomesh-embedded film. Before fabricating the polydimethylsiloxane (PDMS) mould, a Si master mould containing the micro-pattern with a pitch of 10 μm was prepared using photolithography and reactive ion etching process. Then, the surface of the Si master mould was fluorinated using heptadecafluoro-1,1,2,2-tetra-hydrodecyl trichlorosilane to reduce the surface energy and facilitate the following smooth detachment of the PDMS mold.[29]

Department of Materials Science and Engineering, Korea University, Anam-ro 145, Sungbuk-Gu, Seoul, 02841, Republic of Korea. E-mail: heonlee@korea.ac.kr; Fax: +82 2 958 3584; Tel: +82 2 32903284

RSC Advances Accepted Manuscript

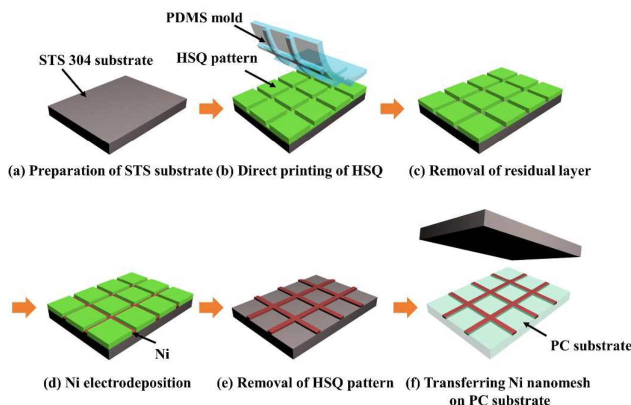

Fig. 1. (Colour online) Schematic illustration of the fabrication process of the Ni-mesh-embedded film.

To fabricate the PDMS mould, Sylgard 184 and its curing agent were mixed in a volume ratio of 10:1. Then, mixed solutions were poured onto the Si master mould and cured at 80 °C for 2 h without air bubbles. After that, the mesh-patterned PDMS mould was physically detached from the Si master mould to use as a flexible mould for direct printing.
Polished 304 stainless steel (STS 304, Alfa Aesar) was prepared as a substrate for Ni electrodeposition (Fig. 1a). To fabricate a template on the STS 304 substrate, hydrogen silsesquioxane (HSQ, Fox-16, Dow Corning), used as a resist, was spin-casted on the PDMS mould at 3000 rpm for 30 s. Subsequently, the HSQ-coated PDMS mould was placed in conformal contact on the STS 304 substrate with a pressure of 5 bar for 5 min. Then, the PDMS mould was detached, and the HSQ-patterned STS 304 substrate was successfully formed, as shown in Fig. 1b. The HSQ-patterned substrate was oxidized using UV/ozone treatment for 30 min to retain the shape, and the residual layer of the HSQ pattern was removed using reactive ion etching process to partially expose the surface of the STS 304 substrate (Fig. 1c). After that, Ni was selectively deposited on the exposed STS 304 substrate using pulsed current electrodeposition, as shown in Fig. 1d. The pulsed current was tuned using a forward current density of 5 mA/cm^2 for 400 ms and reverse current density of 7 mA/cm^2 for 200 ms. After the Ni electrodeposition was conducted, the HSQ pattern was removed using a diluted buffered oxide etchant solution (Fig. 1e). Finally, the Ni nanomesh was embedded into a polycarbonate (PC) film using a hot transfer process (Fig. 1f). Briefly, the Ni-deposited STS 304 substrate and PC film were in contact and then heated over the glass transition temperature, approximately 170 °C, to increase the viscosity of the PC film. Then, a pressure of 20 bar was applied between them to deform the PC film. After the PC film was deformed to match the surface of the Ni-deposited PC film, the temperature was reduced to room temperature, and the STS 304 substrate and Ni-embedded PC film were physically detached.

Characterization

The surface morphologies of various types of samples were examined using field-emission scanning electron microscopy (FE-SEM, Hitachi S-4300). The surface roughness was investigated using atomic force microscopy (AFM, Probes Inc.), and conductive mapping images were obtained. The optical transmittance and sheet resistance of the Ni-embedded PC film were measured using UV-Vis spectroscopy (JASCO V-650) and a four-point system. Bending tests of the Ni-embedded PC film were conducted using a lab-made bending test machine.

3. Results and Discussion

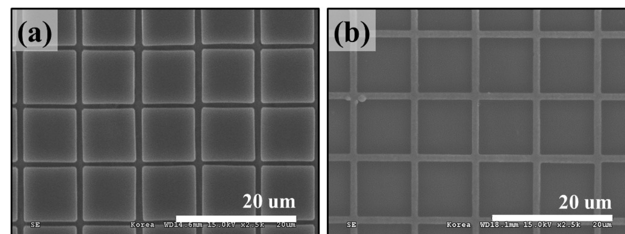

Fig. 2. SEM images of the (a) HSQ-patterned STS 304 substrate and (b) Ni-deposited STS 304 substrate.

Fig. 2a presents a SEM image of the HSQ template pattern on a STS 304 substrate with 10 µm pitch, 9 µm square diameter, and 1 µm height. The HSQ pattern was successfully fabricated on the STS 304 substrate. Then, Ni was selectively deposited on the HSQ-patterned STS 304 substrate to form the Ni nanomesh, as illustrated in Fig. 2b. Ni nanomesh has a pitch of 10 µm and a linewidth of 1 µm. The height of the Ni nanomesh could be easily controlled by tuning the deposition time. Three different heights of Ni nanomeshes were obtained using different deposition times.

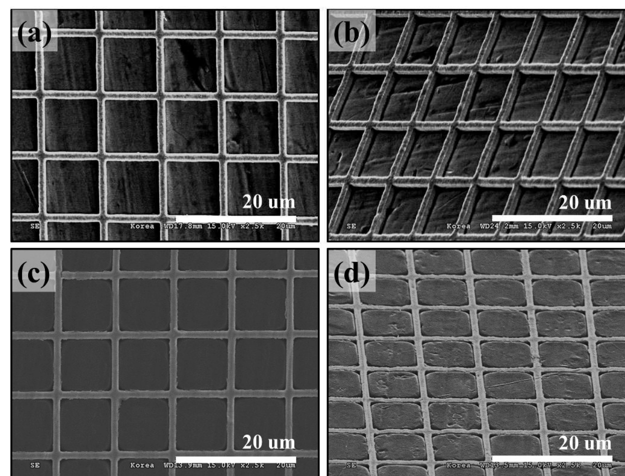

Fig. 3. SEM images of (a) top view and (b) tilted view of the Ni-nanomesh-deposited STS 304 substrate without HSQ pattern and (c) top view and (d) tilted view of the Ni-embedded PC film.

Figs. 3a and 3b present SEM images of the Ni-nanomesh-deposited STS 304 substrate without the HSQ pattern. After removing the HSQ pattern, the surface of the STS 304

RSC Advances Accepted Manuscript

This journal is © The Royal Society of Chemistry 20xx

substrate was examined, which was not perfectly smooth. After the transfer process, the Ni nanomesh was successfully embedded into the PC film, as observed in Figs. 3c and 3d. Compared with Figs. 3a and 3b, the surface roughness of the STS 304 substrate was perfectly transferred onto the PC film during embedding of the Ni nanomesh.

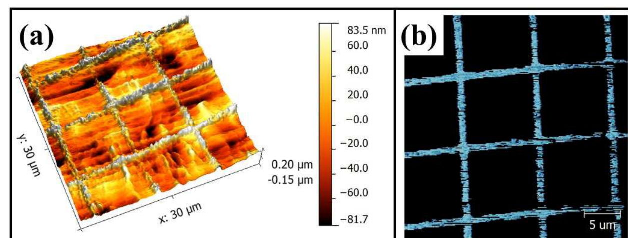

Fig. 4. AFM (a) topography and (b) conductive mode images of for the Ni-embedded PC film.

Fig. 4a presents a topographical image of the Ni-nanomesh-embedded PC film with a height of 500 nm. The surface roughness of the Ni-embedded PC film was measured to be approximately 20 nm. The current flow was also investigated using the conductive mode of AFM, as illustrated in Fig. 4b. In this case, the current flowed through the Ni nanomesh into the PC film without any defects.

Fig. 5a presents a photograph of the Ni-nanomesh-embedded PC film with a height of 300 nm. The Ni nanomesh with an area of 4 cm^2 was successfully embedded into the PC film. The letters underneath the Ni-nanomesh-embedded PC film could be clearly observed through the film.

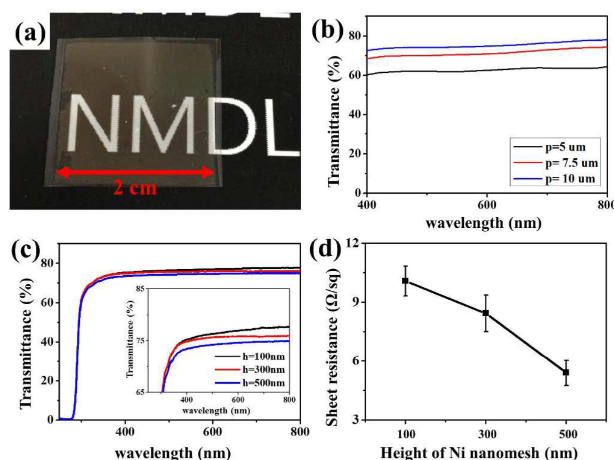

Fig. 5. (a) Photograph of the Ni-embedded PC film and (b) transmittance and (c) sheet resistance of the Ni-nanomesh-embedded PC film for three different heights.

The transmittance of the Ni-nanomesh-embedded PC film was investigated, and the results are presented in Fig. 5b and c. For Ni nanomeshes with three different pitch sizes (pitch = 5 µm, 7.5 µm, and 10 µm; linewidth = 1 µm; height = 100 nm), Fig. 5b presents the total transmittance in the wavelength between 400 nm and 800 nm. The average transmittance of three different Ni-nanomesh-embedded PC films were measured as 63, 73, and 78 % for 5 µm, 7.5 µm, and 10 µm, respectively, if the transmittance of the PC film was set as 100%. This values are slightly lower than the ideal value of the Ni nanomeshes. In the ideal case, the transmittances of 65 %, 75 %, and 81% would be predicted according to the open space of the Ni nanomesh with a pitch of 5 µm, 7.5 µm, and 10 µm and linewidth of 1 µm. The difference was due to the small amount of defects such as over-deposition or an irregular linewidth. Despite of these differences, it was clearly shown that the transmittance of each nanomesh was determined from open space of Ni nanomesh caused by their specific sizes of nanomesh such as pitch and linewidth. Fig. 5c shows the transmittance changes according to height of Ni nanomesh with 10 µm of pitch. For all three different heights of Ni nanomesh, the transmittance was approximately 75% in the visible range that height of Ni nanomesh doesn't significantly affect the total transmittance for normal direction. Fig. 5d shows the sheet resistance of three different heights of Ni-nanomesh-embedded PC films, which have values between approximately 4 to 10 Ω/sq. By increasing the height, the sheet resistance was decreased because of the increase of the cross-sectional area of the Ni nanomesh.

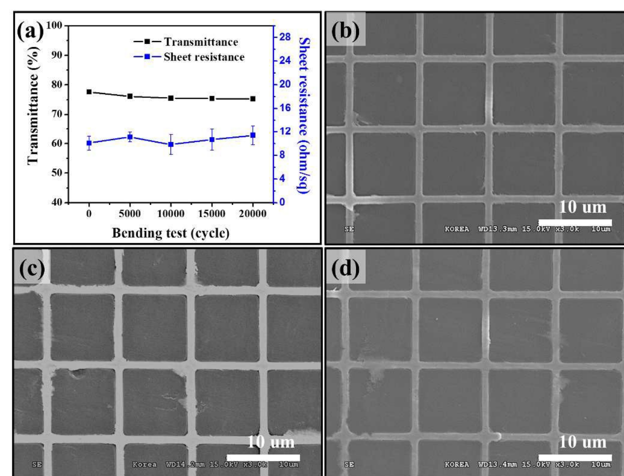

Fig. 6. (a) Optical and electrical properties of the Ni-mesh-embedded film with a height of 100 nm as a function of bending test cycles and SEM images of the Ni-nanomesh-embedded PC film after (b) 5,000, (c) 10,000, and (d) 20,000 cycles.

The electrical properties were sufficient to adapt to various types of electronic devices as an electrode; however, the optical properties were slightly insufficient for application in optoelectronic devices such as solar cells, displays, and light-emitting diodes. It is possible to improve these properties using a master mould with large open space.

Fig. 6a shows the changes in the optical transmittance at a wavelength of 550 nm and the sheet resistance for a Ni-nanomesh-embedded PC film with a height of 100 nm after the bending test. The bending radius of the Ni-embedded PC film decreased from 10 to 3 mm during the bending test. The optical transmittance (~75%) and sheet resistance (~10 Ω/sq)

RSC Advances Accepted Manuscript

Please do not adjust margins

did not significantly change after bending test of 20,000 cycles, which is possible to apply in flexible optoelectronic devices and transparent conducting heater. To confirm the morphological change, the surface of the Ni-nanomesh-embedded PC film was investigated after bending test of 5,000, 10,000, and 20,000 cycles, and the results are presented in Figs. 6b, 6c, and 6d. Significant changes were not observed, which indicates a high durability for bending.

Conclusions

We developed a cost-effective method for fabricating TCEs using template-assisted electrodeposition and a hot transfer process. The height of the Ni nanomesh was easily controlled by tuning the deposition time on a HSQ-patterned template without significant degradation of the optical properties. The Ni nanomesh exhibited semi-transparency (approximately 75%) and a low sheet resistance (below 10 Ω/sq). These values are slightly insufficient for application to optoelectronic devices and transparent micro-heater; however, it is possible to improve the optical properties by adapting a master stamp with a large open space. In addition, high bending resistance was achieved for the Ni-nanomesh-embedded PC film after 20,000 cycles of bending tests, demonstrating its potential application in flexible devices and transparent micro-heater.

Acknowledgements

This research was supported by the Pioneer Research Center Program through the National Research Foundation of Korea funded by the Ministry of Science, ICT & Future Planning (NRF-2013M3C1A3063597).

Notes and references

1 K. Ellmer, Nat. Photonics, 2012, 6, 809.
2 M. W. Rowell, M. A. Topinka, M. D. McGehee, H.-J. Prall, G. Dennler, N. S. Sariciftci, L. Hu and G. Gruner, Appl. Phys. Lett., 2006, 88, 233506.
3 T.-H. Han, Y. Lee, M.-R. Choi, S.-H. Woo, S.-H. Bae, B. H. Hong, J.-H. Ahn and T.-W. Lee, Nat. Photonics, 2012, 6, 105.
4 D. Langley, G. Giusti, C. Mayousse, C. Celle, D. Bellet and J.-P. Simonato, Nanotechnology, 2013, 24, 452001.
5 G. Gruner, J. Mater. Chem., 2006, 16, 3533.
6 B.-Y. Oh, M.-C. Jeong, T.-H. Moon, W. Lee, J.-M. Myoung, J.-Y. Hwang and D.-S. Seo, J. Appl. Phys., 2006, 99, 124505.
7 T. Minami, Thin Solid Films, 2008, 17, 5822.
8 H. Kim, R. C. Y. Auyeung and A. Pique, Thin Solid Films, 2008, 15, 5052.
9 A. Kumar and C. Zhou, ACS Nano, 2010, 4, 11.
10 S. De, T. M. Higgins, P. E. Lyons, E. M. Doherty, P. N. Nirmalraj, W. J. Blau, J. J. Boland and J. N. Coleman, ACS Nano, 2009, 3, 1767.
11 J.-Y. Lee, S. T. Connor, Y. Cui and P. Peumans, Nano Lett., 2008, 8, 689.
12 D. S. Hecht, L. Hu, G. Irvin, Adv. Mater., 2011, 23, 1482.
13 X. Li, Y. Zhu, W. Cai, M. Borysiak, B. Han, D. Chen, R. D. Piner, L. Colombo and R. S. Ruoff, Nano Lett., 2009, 9, 4359.
14 S. Bae, H. Kim, Y. Lee, X. Xu, J.-S. Park, Y. Zheng, J. Balakrishnan, T. Lei, H. R. Kim, Y. I. Song, Y.-J. Kim, K. S. Kim, B. Ozyilmaz, J.-H. Ahn, B. H. Hong and S. Lijima, Nat. Nanotechnol., 2010, 5, 574.
15 H.-Z. Geng, K. K. Kim, K. P. So, Y. S. Lee, Y. Chang and Y. H. Lee, J. Am. Chem. Soc., 2007, 129, 7758.
16 L. Hu, H. S. Kim, J.-Y. Lee, P. Peumans and Y. Cui, ACS Nano, 2010, 4, 2955.
17 H. Guo, N. Lin, Y. Chen, Z. Wang, Q. Xie, T. Zheng, N. Gao, S. Li, J. Kang, D. Cai and D.-L. Peng, Sci. Rep., 2013, 3, 2323.
18 P.-C. Hsu, S. Wang, H. Wu, V. K. Narasimhan, D. Kong, H. R. Lee and Y. Cui, Nat. Commun., 2013, 4, 2522.
19 J. Groep, P. Spinelli and A. Polman, Nano Lett., 2012, 12, 3138.
20 C. F. Guo, T. Sun, Q. Liu, Z. Suo and Z. Ren, Nat. Commun., 2013, 5, 3121.
21 Y. Xia, K. Sun and J. Ouyang, Adv. Mater., 2012, 24, 2436.
22 A. R. Rathmell and B. J. Wiley. Adv. Mater., 2011, 23, 4798.
23 Y. Ahn, Y. Jeong, D. Lee and Y. Lee, ACS Nano, 2015, 9, 3125.
24 P. B. Catrysse and S. Fan. Nano Lett., 2010, 10, 2944.
25 Y.-H. Ho, K.-Y. Chen, S.-W. Liu, Y.-T. Chang, D.-W. Huang and P.-K. Wei, Organ. Electron., 2011, 12, 961.
26 H.-J. Choi, S. Choo, P.-H. Jung, J.-H. Shin, Y.-D. Kim and H. Lee, Nanotechnology, 2015, 26, 055305.
27 Y. Li, Y. Chen, M. Qiu, H. Yu, X. Zhang, X. W. Sun, R. Chen, Sci. Rep., 2016, 6, 20114.
28 B. Y. Ahn, D. J. Lorang and J. A. Lewis, Nanoscale, 2011, 3, 2700.
29 H.-J. Choi, S. Choo, J.-H. Shin, K.-I. Kim and H. Lee. J. Phys. Chem. C, 2013, 117, 24354.

RSC Advances Accepted Manuscript

This journal is © The Royal Society of Chemistry 20xx

Please do not adjust margins